ARTICLE

Compaction and Self-Association of Megabase-Sized Chromatin is Induced by Anionic Protein Crowding

Received 00th January 20xx,
Accepted 00th January 20xx

DOI: 10.1039/x0xx00000x

Anatoly Zinchenko,[a]* Qinming Chen,[b] Nikolay V. Berezhnoy,[b§] Sai Wang,[b#] Lars Nordenskiöld[b]*

Highly compacted chromatin, a complex of DNA with cationic histone proteins, is found in the nucleus of eukaryotic cells in an environment with a high concentration of macromolecular species, many of which possess a negative charge. In the majority of previous studies, however, these crowding conditions were experimentally modelled using neutral synthetic macromolecules such as polyethylene glycol (PEG). Despite the importance of the crowding agent charge in the condensation process of chromatin, to the best of our knowledge, the behavior of chromatin under conditions of anionic protein crowding has not been studied. Here, compaction of nearly megabase-long chromatin in the presence of the anionic globular protein BSA, was investigated by single-molecule fluorescent microscopy (FM). We demonstrate different effects of anionic macromolecular crowder (MMC) on DNA and chromatin, compared to neutral MMCs. While DNA molecules undergo gradual compaction into a globular form in the presence of ca. 20% w/v of BSA, chromatin fibres complete coil to globule transition at a much lower concentrations of BSA (*ca.* 5% w/v). Furthermore, at higher concentrations of BSA in solution (>5% w/v), chromatin fibres self-associate and form large spherical or fibrillar supramolecular microstructures characterized by a high colloidal stability and dynamic intermolecular fluctuations. Formation of such self-organized colloids from chromatin is universal and characteristic for chromatin fibres of various lengths. Our results highlight hitherto underappreciated effect of anionic MMC environment on chromatin higher-order structures that may play an important role in self-organization of chromatin *in vivo*.

1. Introduction

Compaction of double-stranded DNA is an important *in vivo* process closely associated with DNA storage, protection and accessibility of DNA genetic information. DNA compaction has been intensively studied for over 5 decades on various model systems[1, 2] in order to address the complex character of intracellular environment on DNA higher-order structure and functions. Among the prevalent model systems, the DNA behavior under conditions of macromolecular crowding (MMC) has attracted significant interest[3, 4] to model the biological effects of highly concentrated macromolecular species in bacteria and cells. The structure and reactivity of DNA were shown to be strongly affected by MMC.[5-7] To mimic MMC *in vitro*, DNA properties are usually characterized under conditions of a high concentration (20-30%) of neutral polymers such as polyethylene glycol (PEG), in presence of physiological concentrations of salt, which promotes the so-called polymer- and salt induced, or Ψ-condensation. MMC greatly induces DNA compaction even in the absence of multivalent cationic binders[8-10] due to unbalanced osmotic pressure of polymer towards DNA volume and the resulting depletion attraction of DNA segments.[11] The subsequent experimental works have demonstrated a higher efficiency of negatively charged crowders in DNA compaction[12, 13] as well as the opposite salt effect to the neutral crowder.[12, 14]

DNA in nuclei of eukaryotes exist in complexes with cationic histone proteins termed chromatin. Interphase chromatin is organized into cell-type specific chromosome territories inside the cell nucleus[15] occupied by individual chromosomes. Each chromosome territory consists of independent and dynamic topologically associating domains (TAD).[16] In human nuclei, TADs are around one megabase-long chromosomal fragments of several hundred nm in size.[17] The cell nucleus contains many negatively charged macromolecular species such as RNA, the nuclear lamina and various proteins, which make up the nuclear matrix, creating a highly crowded environment surrounding the chromatin. Although the effect of negatively-charged species on DNA higher-order structure has attracted certain attention in the past,[18] chromatin has a number of structural features, such as the presence of cationic histone tails,[19] that alter significantly its electrostatic character compared to DNA. For example, contrary to the repulsive interactions between DNA molecules

[a] *Graduate School of Environmental Studies, Nagoya University, Furo-cho, Chikusa-ku, Nagoya, 464-8601, Japan*
E-mail: zinchenko@urban.env.nagoya-u.ac.jp (AZ)
[b] *School of Biological Sciences, Nanyang Technological University, 60 Nanyang Drive, 637551, Singapore Address here.*
E-mail: LarsNor@ntu.edu.sg (LN)
[§] *Present address: Singapore Center for Environmental Life Sciences Engineering, Nanyang Technological University, 60 Nanyang Drive, 637551, Singapore*
[#] *Present address: Department of Emerging Infectious Diseases, Duke-NUS Medical School, National University of Singapore, 8 College Road, 169857, Singapore*
Electronic Supplementary Information (ESI) available: [details of any supplementary information available should be included here]. See DOI: 10.1039/x0xx00000x

and anionic crowders, the presence of cationic histone tails may cause attractive interactions between chromatin and MMC that provoke higher-order structural changes of chromatin, while the formation of nucleosomes reduces the DNA persistence length and makes nucleosome stacking possible.

Recently, we reconstituted a nearly megabase-long chromatin from giant T4 phage DNA in order to observe the conformational behavior of its single molecule collapse induced by multivalent cations[20] and compaction in solutions of a neutral crowder PEG.[21] We showed that the compaction of chromatin is similar to DNA in terms of efficiency but different in the mechanism. Compaction of DNA proceeds by an all-or-none collapse scenario, while the compaction of chromatin is gradual and proceeds through conformations with partially folded chromatin globules.[21] However, to the best of our knowledge, the compaction behavior of chromatin under the influence of proteins or any negatively charged MMC has not been addressed before. In the present study we therefore investigated the effect of a typical anionic crowder, bovine serum albumin (BSA), on the conformation behavior of nearly megabase-long chromatin fibres.

2. Experimental

2.1 Chemicals

Linear T4GT7 DNA and lambda phage DNA were purchased from Nippon Gene Co. Ltd. (Japan). The molar concentration of DNA is expressed as the concentration of DNA monomer units, nucleotides. The recombinant 62×202 DNA consisting of 62 repeats of 202 bp DNA of the Widom '601' high affinity nucleosome positioning sequence was amplified from a plasmid that was a gift from Daniela Rhodes.[22] The fluorescent dye YOYO-1 was provided by Molecular Probes (Invitrogen, Japan). NaCl and KCl were purchased from Nacalai Tesque Inc. (Japan). Poly(ethylene glycol) (PEG) of average molecular weight 10,000 Da (Sigma-Aldrich, USA), dextran of average molecular weight 40,000 Da, and bovine serum albumin of molecular weight 66,500 Da (BSA) (Fujifilm Wako Pure Chemical Co., Japan) were used without purification. Texas Red™ conjugate of BSA was purchased from Thermo Fisher Scientific (Japan). Tris (tris(hydroxymethyl)- aminomethane) and EDTA-Na_2 (disodium dihydrogen ethylenediamine tetraacetate dihydrate) from Nacalai Tesque (Japan) were used to prepare TE buffer solution (10 mM Tris-HCl, 1 mM EDTA) at pH = 8.

2.2 Preparation of recombinant chromatin.

The coding sequences of recombinant human core histones H2A, H2B, and H3.1 were cloned in the pET21a vector, and the H4 histone coding sequence in the pET3a vector. Each core histone was individually expressed in the *Escherichia coli* BL21(DE3)-pLysS strain, purified from inclusion bodies using size-exclusion and cation-exchange chromatography following the established protocol.[23] The histone octamers (HO) were refolded from the equimolar mixture of core histones, purified using size-exclusion chromatography following established protocol[24] and assessed on SDS-PAGE. Reconstitution of the T4 phage DNA and lambda phage DNA with HO was performed using the salt dialysis approach and assessed as previously described.[20] Only monovalent salt (NaCl) was used for dialysis In the chromatin reconstitution protocol, thus, the reconstituted chromatin fibers do not contain divalent cations that might affect self-association. The 62×202 DNA originally constructed in a PET coco-1 vector obtained from Daniela Rhodes, was sub-cloned to a pUC18 vector. After amplified in Sure2 cells, the purified pUC18_62×202 plasmid was digested by the restriction enzymes EcoRV, DraI, and HaeII. The digested DNA fragments were treated with PEG6000 fractionation and further purified with a Sephacryl S1000 column. Purified 62×202 DNA was reconstituted with HO by salt dialysis following standard protocols as described previously.[25] DNA concentration in samples after chromatin reconstitution was measured with a NanoDrop 2000 UV–Vis spectrophotometer (Thermo Scientific, Delaware, USA) at 25 °C. In this work nucleosome arrays with HO loading of either 50% or 100% were prepared and studied.

2.3 Fluorescence microscopy (FM)

Sample solutions for single molecule observations were prepared by successive mixing of TE buffer, monovalent salt stock solution, YOYO-1 solution, crowder solution, and, after 1 hour of pre-incubation, T4 DNA or chromatin stock solution. The final samples were incubated for additional 1 hour prior to observations at 25 °C. The TE buffer was used for preparation of all stock and sample solutions in this study, including solution of DNA, chromatin, crowders, NaCl, KCl and fluorescent dyes to maintain exactly the same ionic conditions in studied samples. FM observations were performed using an Eclipse TE2000-U (Nikon, Japan) microscope equipped with 100× oil-immersion lens though B-2A filter (Nikon, Japan) for DNA-bound YOYO dye and G-2A filter for Texas Red labeled BSA observations. Fluorescent images were recorded and analyzed using an EB-CCD camera and an Argus 10 image processor (Hamamatsu Photonics, Japan). The long-axis length of DNA molecules was measured using ImageJ 1.52a software (NIH).

3. Results

Long nucleosome arrays partly loaded with histone octamers (HO, *ca.* 50%) and fully loaded (*ca.* 100%, defined as one nucleosome per 200 bp) were reconstituted with T4 DNA as reported earlier;[21] they are referred hereafter as subsaturated and saturated chromatin fibres. T4 DNA, saturated and subsaturated chromatin fibres (all at DNA concentration 0.2 μM) were labeled with the YOYO-1 fluorescent dye (0.04 μM) and their conformational behavior was monitored by fluorescent microscopy (FM) at single-molecule level. In 0.1 M NaCl solution, T4 DNA and chromatin fibres exist as coils exhibiting free Brownian motion (**Figure 1A**). For quantitative characterization, the long-axis length of single DNA and chromatin fibres were measured as the longest distance in their fluorescent profiles.[26] T4 DNA coils are characterized by an average coil size of *ca.* 3.2 μm (**Figure 1B,C**). Complexation of DNA molecules with HO results in wrapping of a part of the DNA chain around the HO,[19] which decreases the observed length of

the chromatin coil; therefore, the subsaturated and the saturated chromatin fibres under the same conditions are more compact, *ca.* 2.2 μm and *ca.* 1.5 μm, respectively (**Figure 1B,C**).

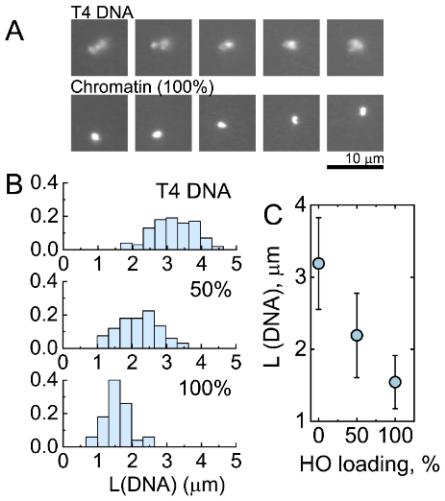

Figure 1. Single-molecule FM observations of conformational changes of T4 DNA and reconstituted chromatin. A. Typical fluorescence micrographs of a YOYO-labeled single T4 DNA molecule and saturated T4 chromatin (100% loading) observed in bulk solution of TE buffer with 0.1 M NaCl. The time interval between snapshots is ca. 0.5 sec. B. Long-axis length distributions of T4 DNA molecules and chromatin at HO loading of 50% and 100% under conditions of A. C. Average long-axis length of T4 DNA and DNA reconstituted with HOs as a function of a loading degree. The error bars indicate the standard deviations of the average values measured over 100 individual DNA or chromatin fibres.

To investigate the influence of an anionic MMC on the conformation of chromatin fibers, a negatively charged globular protein, BSA (M_w 66,500 Da), of *ca.* 10 nm size bearing a −18e charge at neutral pH[27] was used as a crowder. BSA at different concentrations was added to a solution of T4 DNA or chromatin containing physiological concentrations of either NaCl or KCl (0.1 M) and the change of long-axis length of the molecules was recorded (**Figure 2**). The increase of BSA concentration in solutions of T4 DNA or chromatin results in compaction of the molecules (**Figure 2A,B**). The dependences of the average long axis lengths on BSA concentration are shown in **Figure 2C-E**. The compaction of DNA coils begins at BSA concentration above 5% and at 17.5% of BSA only fast-moving globular particles of *ca.* 0.6 μm size are observed, which is in good agreement with the results of past studies.[12] The gradual compaction of chromatin fibres, in contrast to DNA, takes place at lower concentrations of BSA. The complete compaction of subsaturated chromatin is observed at 15% BSA, whereas the saturated chromatin was fully compacted at 5% BSA (**Figures 2D,E**). For comparison, the compaction of saturated chromatin in presence of typical neutral crowders, polyethylene glycol (PEG) and dextran, was performed under similar conditions. Compaction of chromatin in a solution of the flexible PEG polymer (M_w 10,000 Da) is a gradual process which results in the complete compaction of chromatin fibres into globules at much higher PEG concentrations (*ca.* 25%) (**Figure 2F**). A solution of dextran (M_w 40,000 Da) causes only a slight chromatin compaction at dextran concentration up to 20% (**Figure 2G**). Compaction of T4 DNA does not occur in concentrated solutions of dextran (data not shown). The anionic crowder BSA is strikingly more efficient in promoting chromatin compaction than the neutral PEG and dextran.

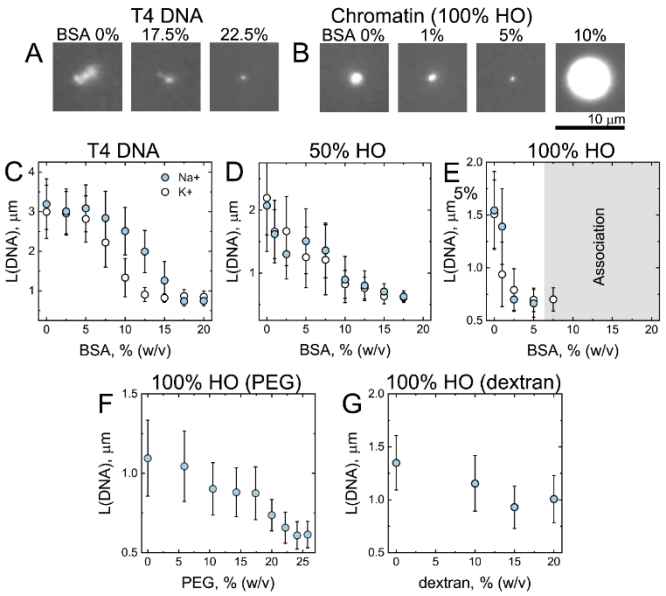

Figure 2. Compaction of T4 DNA and reconstituted chromatin in solution of BSA and 0.1 M NaCl or KCl. A-B. Typical fluorescence micrographs of (**A**) a YOYO-labelled T4 DNA and (**B**) chromatin at 100% HO loading observed at different concentrations of BSA in a bulk solution of TE buffer with 0.1 M of NaCl. The concentrations of BSA are indicated above the corresponding images. **C-E.** Changes in the average long-axis length of (**C**) T4 DNA, (**D**) chromatin at 50%, and (**E**) chromatin at 100% HO loading at various concentrations of BSA in a bulk solution of TE buffer with 0.1 M of NaCl (blue symbols) or 0.1 M KCl (white symbols). The grey area corresponds to self-association of chromatin. **F.** Changes in the average long-axis length of chromatin at 100% HO loading at various concentrations of PEG (M_w = 10,000) in a bulk solution of TE buffer with 0.1 M of NaCl. (reproduced with permission from,[21] Copyright Elsevier 2018) **G.** Changes in the average long-axis length of chromatin at 100% HO loading at various concentrations of dextran (M_w = 40,000) in a bulk solution of TE buffer with 0.1 M of NaCl. The error bars in **C-G** indicate the standard deviations of the average values measured over at least 100 individual T4 DNA or chromatin fibres.

Compaction of saturated chromatin fibres in solution of BSA exhibits a phenomenon, which has not been reported in studies of DNA and chromatin in the presence of neutral MMCs. At higher concentrations of BSA, saturated chromatin fibres self-assemble into several μm long spherical and/or 10-20 μm fibrous intermolecular aggregates (**Figure 3A, right**). Saturated chromatin aggregates begin to appear at 5% of BSA (**Figure 2E**) and coexist with compact chromatin globules. At 7.5% and higher BSA concentrations, only aggregates are observed. Self-assembly of subsaturated chromatin does not happen at the studied concentrations of BSA. Taking into account the concentration of chromatin fibres in the TE buffer without BSA and the number of aggregates in BSA solutions, the aggregates (such as one in **Figure 3A)** can be estimated to contain hundreds of chromatin fibres. The aggregates of chromatin are stable colloidal particles that exhibit free Brownian motion and do not precipitate. Furthermore, these globular and fibrous structures exhibit internal fluctuations. The fluorescence intensities of

Texas Red labeled BSA inside and outside the chromatin aggregates were similar indicating no discernible excess accumulation of BSA in self-assembled particles (**Supporting Information, Figure S1**). The self-assembled aggregates do not exhibit the interfacial droplet-like features and behaviour typical for liquid-liquid phase separation (LLPS) recently also observed for chromatin (**Supporting Information, Figures S1, S2**).[28]

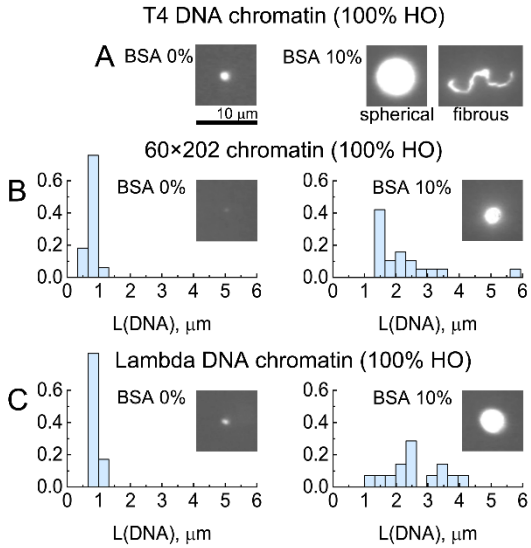

Figure 3. Self-association of chromatin of different lengths at high concentrations of anionic crowder. Typical fluorescence micrographs and size distributions of single chromatin fibres reconstructed from T4 DNA (**A**) 62×202 DNA (**B**), and lambda DNA (**C**) at 100% HO loading and their aggregates observed in bulk solution of TE buffer and 0.1 M NaCl and in the presence of 10% BSA. At least 100 individual chromatin fibres and at least 10 aggregates were used to build histograms. Size distributions of T4 DNA chromatin (**A**) are not displayed because only a few large aggregates of a different morphology (spherical and fibrous) were observed.

The self-assembly of chromatin fibres to spherical aggregates in solution of BSA is independent of the chromatin length. The spherical aggregates were observed in solutions of chromatin reconstituted using 12 kbp (62×202) and 53 kbp (lambda phage) DNA templates in the presence of 10% BSA **(Figures 3B,C)**. The aggregates composed of shorter chromatin fibres are smaller than the T4 DNA-based chromatin aggregates and no fibrillar structures were observed.

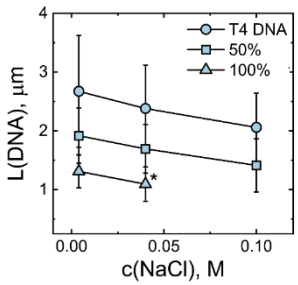

Figure 4. Salt effect in T4 DNA and reconstituted chromatin compaction under anionic MMC. Changes in the average long-axis length of YOYO-labeled T4 DNA and chromatin fibres at 50% and 100% HO loading at various concentrations of NaCl in 10% BSA solution in TE buffer. The error bars indicate the standard deviations of the average values measured over at least 100 individual T4 DNA or chromatin fibres. Asterisk (*) indicates co-existence of aggregates. Data for the 100% HO loaded chromatin at NaCl concentration of 0.1 M are not shown due to chromatin self-association.

Monovalent salt concentration plays a central role in the process of macromolecular phase transitions and can either promote[29] or inhibit[14] DNA compaction in the presence of MMC depending on a charge of a crowder. NaCl, in a concentration range from 4 mM to 0.1 M, was found to promote DNA and chromatin compaction, based on the observed decrease of average long-axis length **(Figure 4)**. In addition to ionic strength, the difference between Na^+ and K^+ in their effect on DNA and chromatin compaction was analyzed (**Figure 2C-E**). The K^+ is more effective than Na^+ in DNA compaction: in the presence of 0.1 M of KCl, full compaction of DNA is observed at 5% lower concentration of BSA (12.5%) in comparison with the NaCl (17.5%) (**Figure 2C**). The difference between Na^+ and K^+ is insignificant in case of chromatin at either 50% or 100% due to compaction occurring in a more narrow range **(Figures 2D,E)**. Interestingly, this correlation is the opposite in the case of DNA[29] and chromatin[21] compaction in the presence of neutral PEG, where Na^+ is more efficient than K^+.

4. Discussion

Based on the results of our study, the scenario of the (saturated) chromatin higher-order structural transition in anionic MMC appears as a compaction from a coil to a globular form accompanied and further dominated by self-assembly into micrometer-sized aggregates (**Figure 5**).

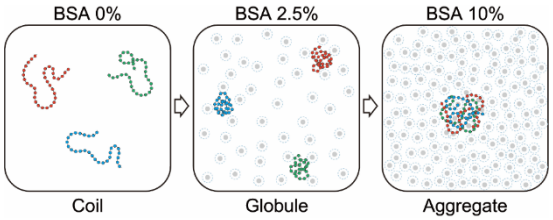

Figure 5. Conformational transition of chromatin at high concentrations of anionic crowder. Schematic illustration of structural transitions for chromatin fibres in presence of the anionic MMC.

The compaction of saturated chromatin fibres in the presence of anionic BSA is markedly different from both DNA compaction in BSA (**Figure 2A**) and from chromatin compaction in the presence of neutral crowders ([21], **Figure 2F,G**): the chromatin compaction in the presence of BSA exhibits a significantly higher efficiency and different morphologies of the compact species.
In order to discuss the mechanism of chromatin compaction in BSA, one should consider two main contributing forces.[4] First, the osmotic pressure that anionic BSA molecules exert on the chromatin compared to neutral crowder molecules, which is primarily related to its excluded volume. To compare the excluded volume, **Table 1** shows molecular weights and hydrodynamic radii of the studied crowders. It is clear that, while the hydrodynamic radii of BSA and PEG molecules are close, the molecular weight of BSA molecule is much larger, and,

consequently, the total excluded volume of BSA is estimated[14] to be *ca.* 6 times smaller than that of PEG at the same w/v concentration. The electrostatic repulsion between the anionic BSA and chromatin fiber results in increase of the excluded volume of BSA and this contribution can be addressed adopting a Debye length.

Table 1. Molecular weights and hydrodynamic radii of the studied crowders.

	BSA	PEG	Dextran
Molecular weight (M_w)	66,500 Da	10,000 Da	40,000 Da
Hydrodynamic radius (R_H)	3.4 nm[30]	3.5 nm[31]	4.8 nm[31]

However, under the experimental conditions of the present study (0.1 M NaCl) the Debye length is only about 1 nm, which roughly doubles the excluded volume of BSA. Consequently, the resulting total excluded volume of BSA is still several times smaller than that of PEG as well as of dextran. Hence, the difference in osmotic pressure of the crowders does not explain the efficient compaction of chromatin in the presence of BSA.

Second, cationic histones neutralize nearly half of the DNA negative charges, and the cationic histone tails promote chromatin compaction by attractive interactions between nucleosomes. Earlier experimental and molecular simulation studies highlighted the important role of chromatin histone tails in chromatin folding via mediating inter-nucleosomal interactions[32] and screening of the electrostatic repulsion between the DNA segments promoting fiber/fiber interactions.[33, 34] Bridging interactions[35] of anionic BSA with cationic sites on chromatin may also promote the chromatin compaction.

Spontaneous self-assembly of chromatin fibres into globular aggregates at concentrations of BSA above 5% deserves particular attention because it has not been demonstrated in studies using neutral MMC with either DNA or chromatin in very diluted regimes[12, 21] (**Figure 2F,G**). Self-organization of 10-nm chromatin fibers has been studied intensively and discussed during past decades due to its relevance in the formation of chromosome territories during interphase[15] and the formation of 0.1 to 10 megabase-long globular structures of TADs.[16, 36] The formation of such structures is interpreted as chromatin assembly in polymer melt-like condensates through long-range interactions,[37] which is supported by a number of experimental works on globular megabase-long chromatin domains.[38] In this regard, recently, Maeshima et al. has demonstrated aggregation of short nucleosome arrays (12-mers) into micrometer-sized supramolecular globular structures[39] in the presence of Mg^{2+} ions. We show that kilobase-sized and sub-megabase-sized nucleosome arrays can self-assemble into similar globular microstructures in the presence of anionic MMC even in the absence of divalent cations (**Figure 3**). This suggests the ability of chromatin to self-assemble as an intrinsic property even at a very low DNA concentrations in the presence of anionic MMC, which implies that this mechanism is viable inside the cell nucleus.

Here it was demonstrated that globular chromatin assemblies as well as fibrous ones can coexist under the same conditions for long nucleosome arrays (**Figure 3A**). We interpret the formation of such structures (**Figure 3**) as a result of the contribution of inter- and intra-molecular attractive nucleosome-nucleosome interactions, which are amplified by the strong depletion interactions caused by the presence of anionic crowders. Insufficient number of such interactions in the subsaturated chromatin results in only a moderate increase of its compaction efficiency compared to DNA and monomolecular compaction scenario. The experiment with fluorescently-labeled BSA indicates the BSA acts mainly as a crowder and not as a component of chromatin aggregates, hence the aggregates do not exhibit the properties of a LLPS phenomenon. The fibrous chromatin aggregates formed *in vitro* resemble interphase chromatin fibers originating from chromatin structure regulator protein knockout or transcription,[40, 41] suggesting that supramolecular chromatin fiber formation is an intrinsic property that can be induced by variety of factors and may represent a chromatin compaction state present in the cell nucleus.

Compaction and aggregation of chromatin fibres is promoted with the increase of ionic strength from millimolar to physiological salt concentrations (**Figure 4**). Considering only crowding effect, the increase in ionic strength should decrease the Debye length of the BSA anionic species and promote DNA and chromatin decompaction due to decrease in the excluded volume of BSA molecules.[12, 14] On the other hand, monovalent counterions screen electrostatic charge on chromatin and BSA molecules that weakens electrostatic interactions. Particularly, higher affinities of Na^+ (relative to K^+) to the negatively charged carboxylate ($-COO^-$, from Asp and Glu amino acids)[42] (and references cited in[42]) and phosphate groups[43, 44] ($-OPO_3^{2-}$; present due to phosphorylation of BSA from natural sources) result in a reduced effective charge on the BSA molecules in the presence of Na^+, making DNA compaction less effective compared to the presence of K^+. To explain the increase of the saturated chromatin compaction efficiency at higher ionic strengths despite the weakening of depletion, we suggest that nucleosome-nucleosome attractive interactions at low salt are less important since histone tails of nucleosome are condensed onto DNA.[32, 34] Partial extension of the cationic tails, which is completed at 50 mM NaCl concentration in aqueous solutions[32] should strengthen the attraction interactions between nucleosomes through bridging[34] thus promoting compaction and association of both subsaturated and saturated chromatin fibres.

BSA is a native protein, and most other proteins found in the cell nucleus have net negative surface charge, intrinsic or due to phosphorylation. This work reproduces known biologically relevant effects of chromatin such as compaction and aggregation in a crowded environment of negatively charged proteins at physiological salt concentrations. While the neutral crowders are not known to be found in nuclei, neutral natural and synthetic polymers were reported to be less effective chromatin compacting agents that do not induce aggregation. Macromolecular crowding with positive charges, such as

dendrimers or peptides, can effectively compact DNA; however highly charged molecules can destroy chromatin,[45] and are known to be generally cytotoxic.

5. Conclusions

This work provides further insights into the compaction scenarios of nearly megabase-long chromatin fibres under influence of MMC. We demonstrate that compaction of chromatin in the presence of high concentrations of macromolecular crowders is strongly affected by the electrostatic charge of the crowder. Compaction of chromatin fibres in the presence of the anionic BSA is substantially more efficient than the compaction of DNA under the same conditions. This difference strongly suggests correlation between chromatin saturation and the extent of chromatin compaction that can help to accommodate large chromatin fibres in a limited nuclear space. Furthermore, compaction of chromatin fibres, both megabase- and kilobase-long, influenced by the anionic MMC results in self-assembly of chromatin fibres into large aggregates that should be of significant relevance and importance for chromatin dynamics *in vivo*.

Conflicts of interest

There are no conflicts to declare.

Acknowledgements

Nikolay Korolev (Nanyang Technological University, Singapore) is acknowledged for insightful discussion. This work was supported by a Singapore Ministry of Education (MOE) Academic Research Fund Tier 1 grant (2018-T1-001-114) and KAKENHI grant 17K05611 from Japan Ministry of Education, Culture, Sports, Science and Technology (MEXT).

Notes and references

1. V. B. Teif and K. Bohinc, *Prog. Biophys. Mol. Biol.*, 2011, **105**, 208-222.
2. A. Zinchenko, *Adv. Colloid. Interface. Sci.*, 2016, **232**, 70-79.
3. M. Yanagisawa, T. Sakaue and K. Yoshikawa, *Int. Rev. Cel. Mol. Bio.*, 2014, **307**, 175-204.
4. R. de Vries, *Biochimie*, 2010, **92**, 1715-1721.
5. L. E. Baltierra-Jasso, M. J. Morten, L. Laflor, S. D. Quinn and S. W. Magennis, *J. Am. Chem. Soc.*, 2015, **137**, 16020-16023.
6. B. Akabayov, S. R. Akabayov, S. J. Lee, G. Wagner and C. C. Richardson, *Nat. Commun.*, 2013, **4**, 1615.
7. C. D. Chapman, S. Gorczyca and R. M. Robertson-Anderson, *Biophys. J.*, 2015, **108**, 1220-1228.
8. U. K. Laemmli, *Proc. Natl. Acad. Sci. USA*, 1975, **72**, 4288-4292.
9. V. V. Vasilevskaya, A. R. Khokhlov, Y. Matsuzawa and K. Yoshikawa, *J. Chem. Phys.*, 1995, **102**, 6595-6602.
10. L. S. Lerman, *Proc. Natl. Acad. Sci. USA*, 1971, **68**, 1886-1890.
11. S. Asakura and F. Oosawa, *J. Chem. Phys.*, 1954, **22**, 1255-1256.
12. M. K. Krotova, V. V. Vasilevskaya, N. Makita, K. Yoshikawa and A. R. Khokhlov, *Phys. Rev. Lett.*, 2010, **105**, 128302.
13. A. Zinchenko, K. Tsumoto, S. Murata and K. Yoshikawa, *J. Phys. Chem. B*, 2014, **118**, 1256-1262.
14. K. Yoshikawa, S. Hirota, N. Makita and Y. Yoshikawa, *J. Phys. Chem. Lett.*, 2010, **1**, 1763-1766.
15. T. Cremer and M. Cremer, *Cold Spring Harb. Perspect. Biol.*, 2010, **2**.
16. J. R. Dixon, S. Selvaraj, F. Yue, A. Kim, Y. Li, Y. Shen, M. Hu, J. S. Liu and B. Ren, *Nature*, 2012, **485**, 376-380.
17. M. Wachsmuth, T. A. Knoch and K. Rippe, *Epigenet. Chromatin*, 2016, **9**.
18. A. Zinchenko and K. Yoshikawa, *Curr. Opin. Colloid Interface. Sci.*, 2015, **20**, 60-65.
19. K. Luger, A. W. Mader, R. K. Richmond, D. F. Sargent and T. J. Richmond, *Nature*, 1997, **389**, 251-260.
20. A. Zinchenko, N. V. Berezhnoy, S. Wang, W. M. Rosencrans, N. Korolev, J. R. C. van der Maarel and L. Nordenskiold, *Nucleic Acids Res.*, 2018, **46**, 635-649.
21. A. Zinchenko, N. V. Berezhnoy, Q. M. Chen and L. Nordenskiold, *Biophys. J.*, 2018, **114**, 2326-2335.
22. V. A. T. Huynh, P. J. J. Robinson and D. Rhodes, *J. Mol. Biol.*, 2005, **345**, 957-968.
23. K. Luger, T. J. Rechsteiner and T. J. Richmond, *Methods Mol Biol*, 1999, **119**, 1-16.
24. N. V. Berezhnoy, D. Lundberg, N. Korolev, C. Lu, J. Yan, M. Miguel, B. Lindman and L. Nordenskiöld, *Biomacromolecules*, 2012, **13**, 4146-4157.
25. A. Allahverdi, R. L. Yang, N. Korolev, Y. P. Fan, C. A. Davey, C. F. Liu and L. Nordenskiold, *Nucleic Acids Res.*, 2011, **39**, 1680-1691.
26. K. Yoshikawa and Y. Matsuzawa, *Physica D: Nonlinear Phenomena*, 1995, **84**, 220-227.
27. T. Peters, *Adv. Protein. Chem.*, 1985, **37**, 161-245.
28. B. A. Gibson, L. K. Doolittle, M. W. G. Schneider, L. E. Jensen, N. Gamarra, L. Henry, D. W. Gerlich, S. Redding and M. K. Rosen, *Cell*, 2019, **179**, 470-484 e421.
29. A. Zinchenko and K. Yoshikawa, *Biophys. J.*, 2005, **88**, 4118-4123.
30. S. K. Chaturvedi, E. Ahmad, J. M. Khan, P. Alam, M. Ishtikhar and R. H. Khan, *Mol. Biosyst.*, 2015, **11**, 307-316.
31. J. K. Armstrong, R. B. Wenby, H. J. Meiselman and T. C. Fisher, *Biophys. J.*, 2004, **87**, 4259-4270.
32. A. Bertin, A. Leforestier, D. Durand and F. Livolant, *Biochemistry-Us*, 2004, **43**, 4773-4780.
33. G. Arya and T. Schlick, *Proc. Natl. Acad. Sci. USA*, 2006, **103**, 16236-16241.
34. N. Korolev, A. P. Lyubartsev and L. Nordenskiöld, *Biophys J*, 2006, **90**, 4305-4316.
35. R. Podgornik and M. Ličer, *Curr. Opin. Colloid Interface. Sci.*, 2006, **11**, 273-279.
36. E. P. Nora, B. R. Lajoie, E. G. Schulz, L. Giorgetti, I. Okamoto, N. Servant, T. Piolot, N. L. van Berkum, J. Meisig, J. Sedat, J. Gribnau, E. Barillot, N. Bluthgen, J. Dekker and E. Heard, *Nature*, 2012, **485**, 381-385.
37. K. Maeshima, S. Ide, K. Hibino and M. Sasai, *Curr. Opin. Genet. Dev.*, 2016, **37**, 36-45.
38. H. Albiez, M. Cremer, C. Tiberi, L. Vecchio, L. Schermelleh, S. Dittrich, K. Kupper, B. Joffe, T. Thormeyer, J. von Hase, S. W. Yang, K. Rohr, H. Leonhardt, I. Solovei, C. Cremer, S. Fakan and T. Cremer, *Chromosome Res.*, 2006, **14**, 707-733.

39. K. Maeshima, R. Rogge, S. Tamura, Y. Joti, T. Hikima, H. Szerlong, C. Krause, J. Herman, E. Seidel, J. DeLuca, T. Ishikawa and J. C. Hansen, *Embo J*, 2016, **35**, 1115-1132.
40. A. Tedeschi, G. Wutz, S. Huet, M. Jaritz, A. Wuensche, E. Schirghuber, I. F. Davidson, W. Tang, D. A. Cisneros, V. Bhaskara, T. Nishiyama, A. Vaziri, A. Wutz, J. Ellenberg and J.-M. Peters, *Nature*, 2013, **501**, 564-568.
41. Y. Hu, I. Kireev, M. Plutz, N. Ashourian and A. S. Belmont, *The Journal of Cell Biology*, 2009, **185**, 87-100.
42. N. Korolev and L. Nordenskiold, *Biomacromolecules*, 2000, **1**, 648-655.
43. H. T. Tien, *J. Phys. Chem*, 1964, **68**, 1021-1025.
44. Y. Xie, Y. Jiang and D. Ben-Amotz, *Anal. Biochem.*, 2005, **343**, 223-230.
45. D. Lundberg, N. V. Berezhnoy, C. Lu, N. Korolev, C.-J. Su, V. Alfredsson, M. d. G. Miguel, B. Lindman and L. Nordenskiöld, *Langmuir*, 2010, **26**, 12488-12492.